



ELSEVIER

Journal of Alloys and Compounds 323–324 (2001) 292–296

Journal of
ALLOYS
AND COMPOUNDS

www.elsevier.com/locate/jallcom

Absorption spectroscopy of Er:GdCOB and Yb:GdCOB crystals

C.S.K. Mak*, P.A. Tanner, Z. Zhuo

Department of Biology and Chemistry, City University of Hong Kong, Tat Chee Avenue, Kowloon, Hong Kong SAR, PR China

Abstract

Polarized electronic absorption spectra are reported for Er³⁺ and Yb³⁺ doped into a gadolinium calcium oxoborate (GdCOB) host. The transitions can be assigned using a model in which the lanthanide ion occupies a single C_s site in the host lattice. The infrared spectra of the host are utilized in the assignment of one- and two-centre vibronic transitions. © 2001 Elsevier Science B.V. All rights reserved.

Keywords: Insulators; Electronic band structure; Optical properties; Light absorption and reflection

1. Introduction

Gadolinium calcium oxoborate, Ca₄GdO(BO₃)₃ (GdCOB), has attractive properties such as a wide optical transparency range, moisture insensitivity, hardness, chemically inertness and the ability to prepare large crystals of excellent optical quality, which enable it to become a good candidate for a novel laser material [1]. It may be synthesized by melting various oxides in stoichiometric proportions, and crystals can be grown by the Czochralski pulling method. The structural details of the isostructural Ca₈Sm₂O₂(BO₃)₆ were first investigated by Khamaganova et al. [2]. The lanthanide atom is coordinated with six surrounding oxygen atoms in a distorted octahedral symmetry. There are two types of Ca atoms situated in the unit cell: one forms a CaO₆ octahedron and the other a CaO₈ polyhedron. Since the replacement of Gd³⁺ in GdCOB provides a suitable lanthanide ion site for activator ions, the properties have been investigated for several dopant ions, including Nd³⁺ [3–5], Yb³⁺ [6], Pr³⁺, Eu³⁺, Yb/Er³⁺ [7], and Tm³⁺ [8]. It has been demonstrated that the Nd³⁺-doped crystal can act as a self-frequency doubling material [9,10].

This work studies two aspects of the doping of lanthanide ions into GdCOB: first, whether the guest ion occupies only Gd³⁺ sites, or/and in addition (charge-compensated) Ca²⁺ sites; and second, whether vibronic sidebands are prominent in the electronic spectra. The optical spectra of Aron et al. [7] and Dominiak-Dzik et al. [8] were taken to indicate the existence of different types of site by the guest lanthanide ion [11]. By contrast,

Mougel et al. indicated that Gd–Ca cation exchange was <3% [12]. The importance of two-centre cooperative vibronic sidebands in the electronic spectra would indicate an effective nonradiative pathway for depopulation of lasing states.

In order to achieve these aims we recorded the absorption spectra of oriented single crystals of Er:GdCOB and Yb:GdCOB at several temperatures between room temperature and 20 K using polarized radiation.

2. Experimental

Ten mol% Er³⁺-doped Er:GdCOB and 10 mol% Yb³⁺-doped Yb:GdCOB crystals were synthesized by the Czochralski method [4] from 99.99% purity lanthanide oxides. The crystals were cut with orthogonal axes parallel to the *X, Y, Z* crystallophysic axes, where *b*||*Y*, (*a, Z*) ~ 27° and (*c, X*) ~ 16° [4]. The polarized absorption spectra of Er:GdCOB and Yb:GdCOB were recorded by a Biorad FTS-60A wide range spectrometer equipped with PbSe and photomultiplier detectors. The sample was housed in an Oxford Instruments closed cycle cooler cryostat. The IR spectrum of the host lattice was recorded by a Perkin-Elmer PE1600 FTIR spectrometer in the range 500–4000 cm⁻¹ for the pure GdCOB crystal and for a KBr disc.

3. Infrared spectra of the GdCOB host

The highest energy vibrational modes in GdCOB arise from the three nonequivalent borate groups in the Bravais cell. The parent planar BO₃ moiety has four (A₁' + A₂' +

*Corresponding author.

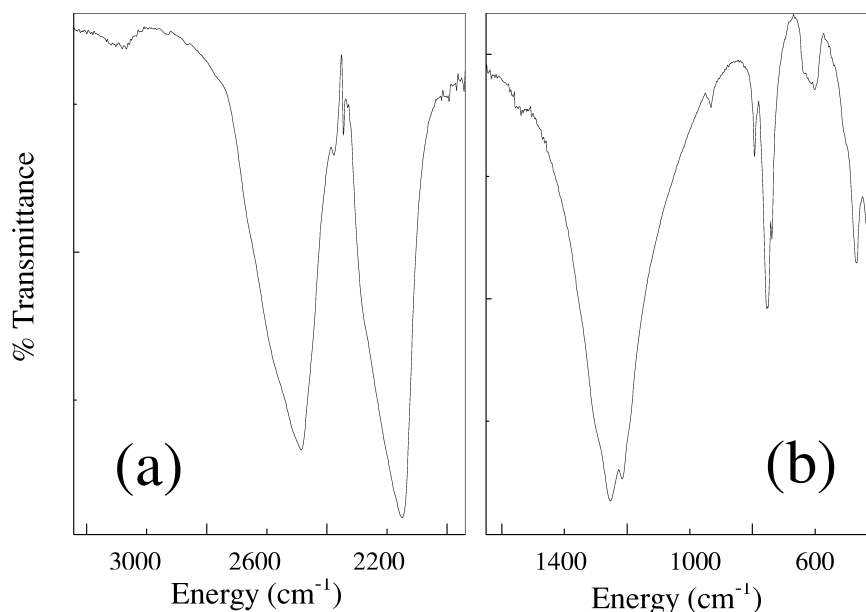


Fig. 1. 300 K infrared spectra of (a) a GdCOB crystal between 2000 and 3500 cm^{-1} ; and (b) a KBr disc of GdCOB between 400 and 1600 cm^{-1} . The scale in (a) is expanded by a factor of 30.

$2E'$) modes of vibration, two of which are degenerate and infrared-active. In the GdCOB crystal, these vibrations transform as $A(C_1)$ site modes, and as nondegenerate infrared-active modes in the C_s unit cell group. The 300 K infrared spectra of Er:GdCOB and Yb:GdCOB were similar for both crystals and were assigned to vibrational transitions of the host lattice. Band splittings were more clearly resolved at 90 K. The fundamental vibrations occur below 1500 cm^{-1} , and are associated with parent three-coordinated boron modes at 1300–1190 cm^{-1} (ν_3 , B–O antisymmetric stretch), 930–940 cm^{-1} (ν_1 , B–O symmetric stretch), 750–795 cm^{-1} (ν_2 , out-of-plane bend), and 605–640 cm^{-1} (ν_4 , BO_3 deformation). The ν_3 mode is intense whereas ν_1 is weak (Fig. 1b). The strong features between 340 and 510 cm^{-1} correspond to Ca–O and Gd–O stretching modes. The higher energy, combination/overtone bands observed in the single crystal spectra (Fig. 1a) are assigned to $\nu_1 + \nu_3$ (2150 cm^{-1}) and $2\nu_3$ (2486 cm^{-1}), respectively.

4. Electronic spectra of Yb^{3+} in a Yb:GdCOB crystal

The electronic ground state of Yb^{3+} in octahedral symmetry is the Kramers doublet ${}^2F_{7/2}\Gamma_6$, the degeneracy of which is not removed at the C_s crystal site in GdCOB. Electronic transitions are possible to the excited term ${}^2F_{5/2}$, for which the lowest level, $\Gamma_8(\text{O}_h)$, splits into two Kramers doublets in GdCOB, $2(\Gamma_3 + \Gamma_4)$ (C_s), whilst the upper level from $\Gamma_7(\text{O}_h)$ is a Kramers doublet. The transition from the electronic ground state to the lower level is both magnetic dipole (MD) and electric quadrupole

(EQ) allowed in octahedral symmetry, whilst that to the upper level is EQ allowed. At the Yb^{3+} C_s site, however, electric dipole (ED) intensity is introduced into these transitions since the inversion centre is lost.

Fig. 2 shows the electronic absorption spectrum of Yb:GdCOB at room temperature and 20 K. The two lowest energy bands at 20 K (at $I=10\,242\text{ cm}^{-1}$, $II=10\,258\text{ cm}^{-1}$) are strongly polarized in perpendicular orientations of the electric vector (as shown in the inset) and are assigned to the C_s components of the parent ${}^2F_{5/2}\Gamma_8(\text{O}_h)$ state. At room temperature, some structure appears to low energy of the zero phonon lines. This structure, to low energy of 10 200 cm^{-1} , is enlarged in Fig. 2. The change in relative intensity is consistent with that calculated from the Boltzmann factors for the corresponding Stokes vibronic structure. This Stokes structure between 10 400 and 10 900 cm^{-1} is complex, but falls into two structured groups of bands, with a bandgap between them. The two groups are also shown on an expanded scale in Fig. 2. The lower group of bands is assigned to O–Yb–O bending, and the upper group to one-centre vibronic transitions involving Yb–O stretching modes, mixed with two-centre oxygen-stretching modes. The feature at 10 855 cm^{-1} (i.e. 613 cm^{-1} above the zero phonon line) is associated with the ν_4 borate bending mode.

An intense, broad band located at 11 107 cm^{-1} at 20 K is assigned to the transition to the upper Kramers doublet level (III), corresponding to the parent $\Gamma_7(\text{O}_h)$ level. Two high energy shoulders correspond to the resonance with the ν_1 borate mode based upon the two lowest energy zero phonon lines, I and II (i.e. ν_1 energy ca. 920 cm^{-1}). The highest energy borate mode, ν_3 , is then assigned to the feature peaking at 11 457 cm^{-1} (about 1215 cm^{-1} from I,

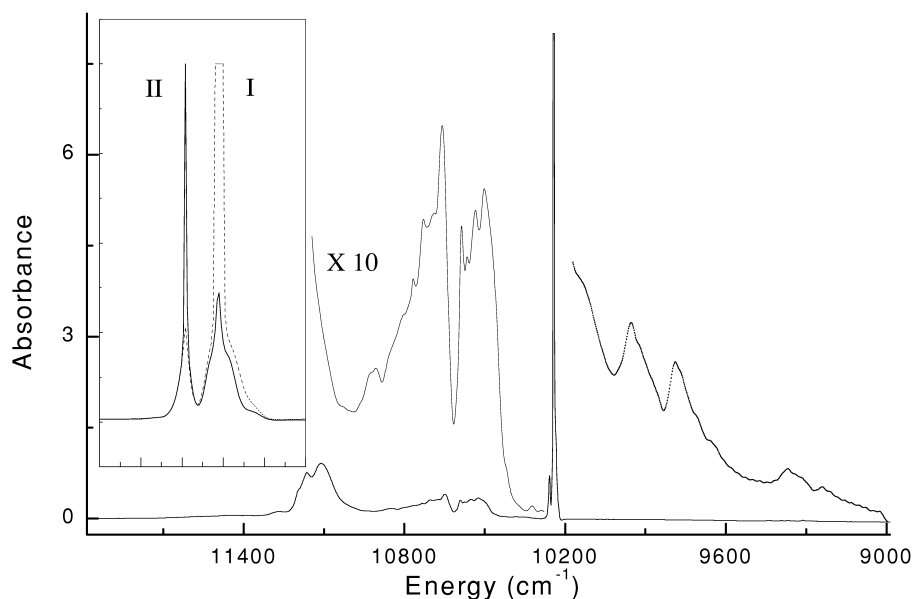


Fig. 2. 20 K absorption spectrum of Yb:GdCOB between 9000 and 12 000 cm^{-1} . The expanded scale line to a low energy of 10 200 cm^{-1} shows the 300 K hot bands. The inset shows the zero phonon lines I and II at 10 242 and 10 258 cm^{-1} for radiation propagating along the X crystallographic axis, with the electric vector at (—) 45° and ($\cdot\cdot\cdot$) 135° to Z. The apparent low energy shoulder on I is not observed in the unpolarized spectra.

II), which overlaps with a structure based upon the origin III. To high energy, a band at 12 324 cm^{-1} (not shown in Fig. 2) is at 1217 cm^{-1} above III, but other weak bands in the region 12 400–13 650 cm^{-1} are associated with a trace Nd^{3+} impurity in the crystal. We have observed similar Nd^{3+} impurity bands in the absorption spectra of other lanthanide ions [13].

5. Electronic spectra of Er^{3+} in a Er:GdCOB crystal

The electronic spectra of Er:GdCOB are much more complicated than those of Yb:GdCOB. This is due to the much larger number of excited multiplet terms of Er^{3+} , and also because the ground state for the Er^{3+} ion is $^4\text{I}_{15/2} \Gamma_8(\text{O}_h)$, which splits into two closely separated (by 22 cm^{-1}) Kramers doublets when diluted into the GdCOB host. Other low-lying states, located at 35, 41 and 64 cm^{-1} , confuse the interpretation by contributing transitions even at low temperatures, which cause further overlapping bands. The simplest electronic transition for analysis is $^4\text{I}_{15/2} \rightarrow ^4\text{S}_{3/2}$, because the $\Gamma_8(\text{O}_h)$ excited state is expected to split into only two Kramers doublet levels. At the Er^{3+} C_s site, the band intensities arise from a combination of EQ, MD and ED mechanisms, and we do not attempt to model them here.

Fig. 3a,b shows unpolarized spectra of this transition at 300 and 35 K, for radiation propagating along different crystallographic axes. The features can be assigned to transitions terminating in two levels at 18 250 and 18 336 cm^{-1} , and originating from several ground state crystal

field levels. Fine structure is resolved for the broader band at 18 336 cm^{-1} , which is assigned to resonances with excited vibronic levels of the lower energy state. Fig. 3c shows the detailed polarization characteristics of this transition.

Vibronic bands associated with $^4\text{I}_{15/2} \rightarrow ^4\text{S}_{3/2}$ are relatively weak, and masked by the intense $^4\text{I}_{15/2} \rightarrow ^2\text{H}_{11/2}$ transition at high energy. The room temperature bands above 18 500 cm^{-1} are hot bands of $^4\text{I}_{15/2} \rightarrow ^2\text{H}_{11/2}$.

6. Conclusions

The electronic absorption spectra of Yb:GdCOB and Er:GdCOB have been rationalized as pure electronic and vibronic transitions by the lanthanide ions occupying a single C_s site in the host lattice. This is in contrast to previous spectral results [8] and interpretations [11], but is consistent with refinement of the X-ray crystal structure [12], which indicated a low degree of disorder in the crystal. Recently, Aron et al. presented evidence from the emission spectrum of Eu:GdCOB showing that the quality of the material determines the form of spectrum obtained [7]. In the stronger crystal field of oxide ligands in Yb:GdCOB, the splitting of the $^2\text{F}_{5/2}$ excited state (865 cm^{-1}) is greater than for chloride ligands (e.g. 470 cm^{-1} in YbCl_6^{3-} [14]), and much greater than in Yb:YAG. The large crystal field splitting of the ground state $^2\text{F}_{7/2}$ term provides broad tunability for this laser material [15].

Vibronic structure is observed clearly in the electronic spectrum of Yb:GdCOB, but is much less prominent in the more congested spectrum of Er:GdCOB. In the GdCOB

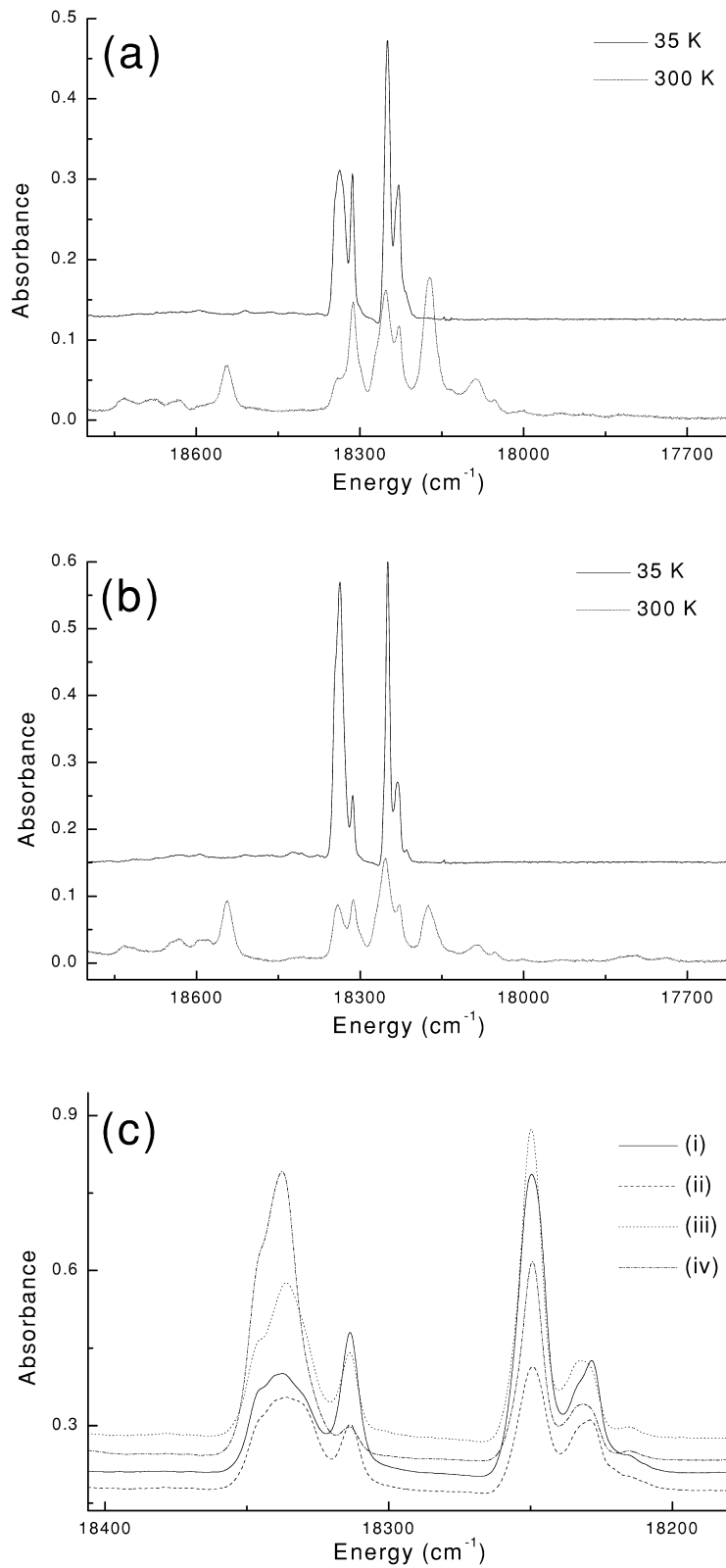


Fig. 3. Absorption spectra of the ${}^4I_{15/2} \rightarrow {}^4S_{3/2}$ transition of Er:GdCOB: 300 and 35 K unpolarized spectra with radiation incident along (a) the Y crystallographic axis, and (b) along X; (c) 35 K polarized spectra with radiation propagating along Y, with the electric vector at (i) 45°, (ii) 135° to Z, and with propagation along X with the electric vector at (iii) 45°, (iv) 135° to Z.

host, nonradiative depopulation of the $\text{Er}^{3+} {}^4\text{I}_{13/2}$ level and of the $\text{Yb}^{3+} {}^4\text{F}_{5/2}$ level requires at least five and eight phonons, respectively. This is not expected to greatly reduce the luminescence efficiency of these levels [16]. However, the presence of trace lanthanide impurities (such as Nd^{3+} , as found herein) may reduce the laser efficiency by nonradiative cross-relaxation pathways.

Acknowledgements

We acknowledge financial support from the City University SRG 7000762.

References

- [1] G. Aka, A. Kahn-Harari, F. Mougél, D. Vivien, F. Salin, P. Coquelin, P. Colin, D. Pelenc, J.P. Damelet, *J. Opt. Soc. Am. B* 14 (1997) 2238.
- [2] T.N. Khamaganova, V.K. Trunov, B.F. Dzhurinskii, *Russ. J. Inorg. Chem.* 36 (1991) 484.
- [3] F. Mougél, G. Aka, A. Kahn-Harari, H. Hubert, J.M. Benitez, D. Vivien, *Opt. Mater.* 8 (1997) 161.
- [4] S. Zhang, Z. Cheng, J. Han, G. Zhou, Z. Shao, C. Wang, Y.T. Chow, H. Chen, *J. Cryst. Growth* 206 (1999) 197.
- [5] F. Mougél, F. Augé, G. Aka, A. Kahn-Harari, D. Vivien, F. Balembois, P. Georges, A. Brun, *Appl. Phys. B* 67 (1998) 533.
- [6] F. Augé, F. Balembois, P. Georges, A. Brun, F. Mougél, G. Aka, A. Kahn-Harari, D. Vivien, *Appl. Opt.* 38 (1999) 976.
- [7] A. Aron, P.Y. Tigréat, A. Caramanian, E. Antic-Fidancev, B. Viana, G. Aka, D. Vivien, *J. Lumin.* 87–89 (2000) 611.
- [8] G. Dominiak-Dzik, W. Ryba-Romanowski, S. Golab, A. Pajaczkowska, *J. Phys. Condens. Matter* 12 (2000) 5495.
- [9] D. Vivien, F. Mougél, G. Aka, A. Kahn-Harari, D. Pelenc, *Laser Phys.* 8 (1998) 759.
- [10] F. Mougél, K. Dardenne, G. Aka, A. Kahn-Harari, D. Vivien, *J. Opt. Soc. Am. B* 16 (1999) 164.
- [11] A.B. Ilyukhin, B.F. Dzhurinskii, *Russ. J. Inorg. Chem.* 38 (1993) 917.
- [12] F. Mougél, A. Kahn-Harari, G. Aka, D. Pelenc, *J. Mater. Chem.* 8 (1998) 1619.
- [13] P.A. Tanner, M.D. Faucher, T.C.W. Mak, *Inorg. Chem.* 38 (1999) 6008.
- [14] P.A. Tanner, V.V.R.K. Kumar, C.K. Jayasankar, M.F. Reid, *J. Alloys Comp.* 215 (1994) 349.
- [15] L. Shah, Q. Ye, J.M. Eichenholz, D.A. Hammons, M. Richardson, B.H.T. Chai, R.E. Peale, *Opt. Commun.* 167 (1999) 149.
- [16] P.A. Tanner, *Chem. Phys. Lett.* 145 (1988) 134.